Bioinspired Hydrogen Bond Motifs in Ligand Design: The Role of Noncovalent Interactions in Metal Ion Mediated Activation of Dioxygen

A. S. BOROVIK
Department of Chemistry, University of Kansas, Lawrence, Kansas 66045

Received May 27, 2004

ABSTRACT

Hydrogen bonds influence secondary coordination spheres around metal ions in many proteins. To duplicate these features of molecular architecture in synthetic systems, urea-based ligands have have been developed that create rigid organic frameworks when bonded to metal ions. These frameworks position hydrogen bond donors proximal to metal ion(s) to form specific chemical microenvironments. Iron(II) and manganese(II) complexes with constrained cavities activate O_2, yielding M^{III} (M^{III} = Fe and Mn) complexes with terminal oxo ligands. Installation of anionic sites within the cavity assists the formation of complexes with $M^{II/III}$−OH and M^{III}−O units derived directly from water. Opening the cavity promotes M(μ-O)$_2$M rhombs, as illustrated by isolation of a cobalt(III) analogue, the stability of which is promoted by the hydrogen bonds surrounding the bridging oxo ligands.

Introduction

Metalloproteins perform a wide range of chemical transformations, most of which have yet to be achieved by synthetic systems.[1−3] The range in function is partially attributed to the unique properties found in metal-containing active sites. From a structure/function perspective, active sites serve two general roles: (1) they provide the necessary ligands to connect the metal ion cofactors to proteins, thereby defining the primary coordination sphere of the metal centers, and (2) they control the secondary coordination sphere (microenvironment) around the metal ion(s). It is well established that the primary coordination sphere impacts many properties of metal complexes, including electronic structure and Lewis acidity. Moreover, the ability of proteins to stabilize metal complexes with unusual coordination geometries or coordinatively unsaturated metal centers is an essential prerequisite for many functions.

Reproducing properties associated with the primary coordination sphere in metalloproteins has led to accurate structural and spectroscopic synthetic models for metal centers within active sites.[4] However, while notable advances have been achieved, most synthetic analogues do not duplicate protein function at room temperature, in part because of their inability to regulate the secondary coordination sphere. Structural and spectroscopic studies on a variety of different proteins have shown that control of the secondary coordination sphere is strongly correlated with function.[5] The chemical microenvironment surrounding metal ions results from the placement of functional groups in precise locations within the active sites.

Hydrogen bonds (H-bonds) are the most common type of interactions used by biomolecules to control the microenvironment around metal ions. These interactions are relatively weak in the condensed phase, having bond strengths ranging from 5 to 15 kcal/mol,[6] yet in many metalloproteins H-bonds are used in conjunction with metal−ligand covalent bonds to control activity. H-bonds are found in heme proteins, such as hemoglobin, cytochrome P450, and horseradish peroxidase (Figure 1).[7−13] The structural biology for non-heme metalloproteins is not as well-defined, yet H-bonds have been correlated to function in superoxide dismutases,[14−16] lipoxygenases,[17] (Figure 2), and methane monooxygenase.[18]

These findings show that H-bonds affect an array of biochemical transformations. Also evident is that the incorporation of these types of interactions into synthetic compounds could lead to systems with new or improved functions. Thus one challenge in synthetic bioinorganic chemistry is the development of complexes having *intra*molecular H-bond(s) that assist chemical transformations. Unlike in protein active sites, difficulties arise in synthetic systems because their structures are often flexible, so H-bonds form with various other species present within the chemical milieu, such as solvent molecules or counterions. These *inter*molecular H-bonds are often unwanted and interfere with the desired function. Therefore, as in metalloproteins, synthetic complexes must have H-bond donors/acceptors placed within rigid frameworks located near the metal center(s) to ensure intramolecular H-bonds.

The structural requirements leading to intramolecular H-bonds have led to the development of polydentate ligands possessing a range of organic frameworks that incorporate H-bond donors/acceptors. These include porphyrins[19−21] and non-heme ligands that are used in recognition processes.[22−24] Examples relevant to the systems discussed in this Account are ligands with H-bond donors appended from pyridyl,[25−27] pyrazolyl,[28,29] and imidazolyl[30] moieties. We have designed systems using principles of molecular architecture outlined for metalloproteins to study the role of H-bonds in metal-based chemical transformations. We reasoned that synthetic systems incorporating these noncovalent effects would allow access to new types of metal complexes or isolation of species that are generally unstable at room temperature. This Account describes our work on 3d transition metal complexes with rigid H-bond frameworks and their reactivity with dioxygen.

A. S. Borovik was raised in Chicago, attended Humboldt State University (B.S., 1981) and the University of North Carolina−Chapel Hill (Ph.D. with Tom Sorrell, 1986), and held postdoctoral positions with Larry Que at the University of Minnesota (1986−1988) and Ken Raymond at the University of California-Berkeley (1990−1992). He has been on the faculty at Ithaca College, Kansas State University, and the University of Kansas, where he is currently a professor.

10.1021/ar030160q CCC: $30.25
Published on Web 12/04/2004

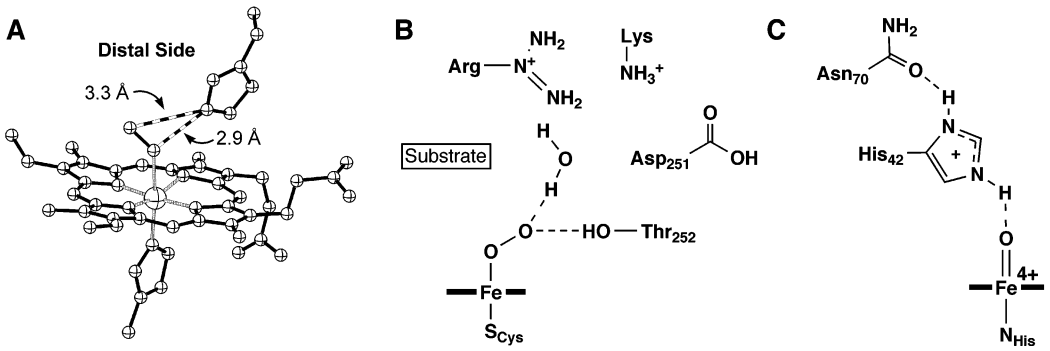

FIGURE 1. Active site structure for oxyhemoglobin (A) derived from X-ray diffraction and proposed H-bonds in the active sites of cytochrome P450 (B) and HRP (C).

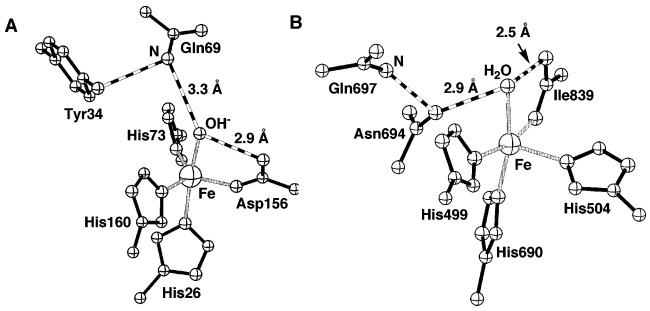

FIGURE 2. Active sites of $Fe^{III}(OH)$SOD (A) and $Fe^{II}(OH_2)$ lipoxygenase (B).

Design Criteria

Figure 3 illustrates key design features of our initial system, tris[(*N*′-*tert*-butylureayl)-*N*-ethylene]amine (H_6buea). This compound has 3-fold symmetry with three *N*-ethylene-*N*′-*tert*-butylurea groups radiating from an apical nitrogen atom. Urea groups were chosen because of their propensity to form H-bonds and their relatively high N−H bond dissociation energies (>100 kcal/mol in DMSO),[31] which we assumed was sufficient to withstand oxidation. The function of the ureas in the system differs from the norm because the two NH moieties, denoted αNH and α′NH, serve different roles within a metal complex. Coordination of a metal ion requires the αNH groups to be deprotonated, producing the trianionic ligand $[H_3buea]^{3-}$, that binds a metal ion at the three αN^- sites and the apical amine nitrogen.

The remaining portions of the urea groups serve as scaffolds for a cavity that surrounds the coordinatively unsaturated metal center. The ureayl scaffolds are positioned nearly perpendicular to the trigonal plane produced by the αN atoms, an arrangement that is supported by the five-membered chelate rings formed upon metal coordination. The resulting cavity is rigid and relatively constrained with the α′NH groups, which remain protonated, positioned inside the cavity. A maximum of three intramolecular H-bonds can form between another ligand (e.g., OH^-, O^{2-}) within the cavity and the α′NH groups of $[H_3buea]^{3-}$. The likelihood of intramolecular H-bonds is reinforced by formation of thermodynamically favored six-membered rings, which should aid in stabilizing these noncovalent interactions. Furthermore, this design relies on the confinement of ligands within the H-bond cavity, which is enhanced by using bulky R groups. The tripodal ligand, $[H_3buea]^{3-}$, is distinct from other ligands because it combines a highly electron-rich metal binding site with the ability to H-bond to other ligands. Deprotonated ureas should aid in the activation of dioxygen through generation of high valent metal intermediates, similar to reactivity observed for complexes with amidate ligands.[32,33]

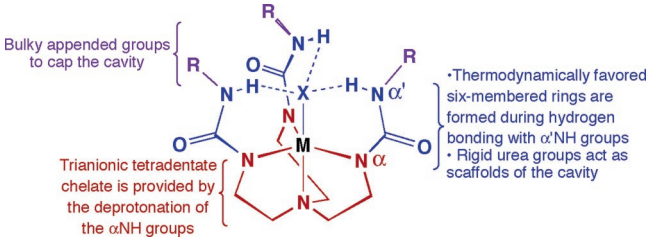

FIGURE 3. Design aspects for C_3-symmetric H-bonding systems.

Dioxygen Activation by Non-Heme Metal Species

We have investigated the influence of H-bonds on the activation of dioxygen with synthetic Fe^{II} and Mn^{II} complexes. Studies on metalloproteins suggested that H-bond donors placed strategically within a metal complex could lead to the new metal−oxygen species, including those with terminal oxo ligands. We anticipated that the protective H-bond cavity of the $[H_3buea]^{3-}$ would sufficiently protect oxometal units to prevent formation of complexes with M−O−M motifs, the usual products from reacting synthetic iron(II) and manganese(II) complexes with dioxygen. Prior to our work, the ferrate ion, FeO_4^-, was the only report of a stable iron complex with a terminal oxo ligand.[34] More recently, Que reported the isolation of six-coordinate Fe^{IV}=O complexes, and the molecular structure for one of these complexes was determined by X-ray diffraction methods.[35] Note that these complexes were prepared using sources other than dioxygen. However, dioxygen activation to form intermediary iron-oxo species is proposed in an array of non-heme metalloproteins,[36] many of which contain monomeric, high-spin ferrous active sites that react with dioxygen.

Scheme 1. Preparative Routes and Molecular Structures for $[Fe^{III}H_3buea(O)]^{2-}$ and $[Fe^{III}H_3buea(OH)]^{-}$ [a]

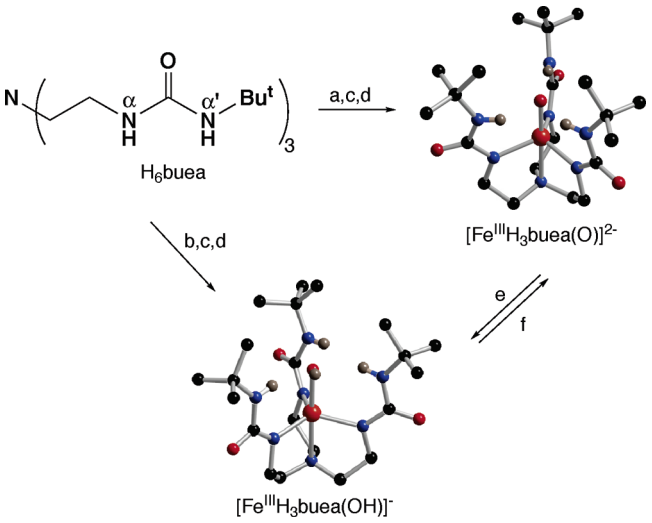

[a] Potassium counterions have been omitted. Conditions: (a) 4 equiv KH, DMA, inert atmosphere (Ar), rt; (b) 3 equiv KH, DMA, Ar, rt; (c) $Fe(OAc)_2$, DMA, Ar, rt; (d) 0.5 equiv O_2, DMA, rt; (e) H^+,DMA rt; (f) base, DMA, rt.

Formation of $[Fe^{III}H_3buea(O)]^{2-}$ and $[Fe^{III}H_3buea(OH)]^{-}$

Scheme 1 illustrates the synthetic procedures used to isolate $[Fe^{III}H_3buea(O)]^{2-}$ and $[Fe^{III}H_3buea(OH)]^{-}$.[37,38] Both complexes were prepared from Fe(II) precursors generated in dimethylacetamide (DMA) and 0.5 equiv of dioxygen. The formation of these complexes is dependent on the amount of base initially added to deprotonate H_6buea. Four equivalents of base were necessary to isolate $[Fe^{III}H_3buea(O)]^{2-}$, whereas 3 equiv of base afforded $[Fe^{III}H_3buea(OH)]^{-}$ as the product. $[Fe^{III}H_3buea(O)]^{2-}$ is converted to $[Fe^{III}H_3buea(OH)]^{-}$ in the presence of 1 equiv of acid (i.e., phenols or water) and to $[Fe^{III}H_3buea(OMe)]^{-}$ when treated with 1 equiv of methyl iodide. These results show the nucleophilic character of the coordinated oxo group, as expected for the terminal oxo ligand coordinated to an iron(III) center.

Dioxygen as the source of the oxo ligand in $[Fe^{III}H_3buea(O)]^{2-}$ was confirmed using $^{18}O_2$ in the reaction sequence shown in Scheme 1. The $\nu(Fe^{16}O)$ band appearing at 671 cm^{-1} shifts to 645 cm^{-1} in $[Fe^{III}H_3buea(^{18}O)]^{2-}$. Similarly, the O-atom of the OH group in $[Fe^{III}H_3buea(OH)]^{-}$ originates from O_2: $[Fe^{III}H_3buea(^{16}OH)]^{-}$ displays a $\nu(^{16}OH)$ = 3632 cm^{-1}, which shifts to 3621 cm^{-1} in the ^{18}O-isotopomer.

Mechanistic Aspects

A proposed mechanism for the formation of $[Fe^{III}H_3buea(O)]^{2-}$ is shown in Figure 4.[37,38] A trans-peroxo-bridged species is consistent with the 1:2 ratio of O_2 to Fe^{II} precursor. Homolysis of the O−O bond produces an Fe^{IV}=O intermediate that is sufficiently confined within the H-bond cavity to prevent reactions with other hindered iron complexes. The Fe^{IV}=O species, however, is competent to abstract an H-atom from external reagents, such as solvent, to produce an Fe^{III}−OH species. If this

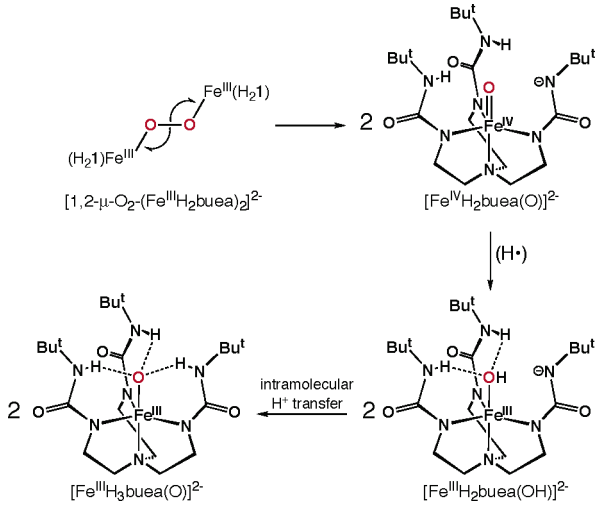

FIGURE 4. Proposed mechanism for the formation of $[Fe^{III}H_3buea(O)]^{2-}$.

species has a basic site positioned near the coordinated hydroxo ligand, we suggest that intramolecular proton transfer occurs between the coordinated hydroxo ligand and the basic site to form the Fe^{III}−O product, $[Fe^{III}H_3buea(O)]^{2-}$.

Two aspects of this mechanism have been explored: (1) the formation of an Fe^{IV}=O intermediate and (2) the deprotonation of an Fe^{III}−OH intermediate with an internal basic site. To probe the former, $[Fe^{III}H_3buea(O)]^{2-}$ has been obtained by treating Fe^{II} precursor, $[Fe^{II}H_2buea]^{2-}$, with oxygen-atom transfer reagents, such as *N*-oxides, sulfoxides, and hydroxylamine (denoted XO in Figure 5). $[Fe^{III}H_3buea(O)]^{2-}$ and the organic product (X) are obtained in satisfactory yields: examples include morpholine *N*-oxide → morpholine (70%), pyridine *N*-oxide → pyridine (70%), and Ph_2S=O → Ph_2S (65%). These results show the strong oxophilic character of the iron complexes generated with the $[H_2buea]^{4-}$ ligand. Furthermore, it provides indirect evidence for the participation of an Fe^{IV}=O intermediate in the formation of $[Fe^{III}H_3buea(O)]^{2}$. The transfer of the oxo group to $[Fe^{II}H_2buea]^{2-}$ would probably first form an Fe^{IV}=O intermediate, which is prone to abstract an H atom. This idea is supported by the large O−H bond dissociation energy (BDE_{OH})[39] of 115 kcal/mol found for $[Fe^{III}H_3buea(OH)]^{-}$, indicating that an Fe^{IV}=O species would have a strong thermodynamic driving force to form an Fe^{III}−OH complex (vide infra).[40]

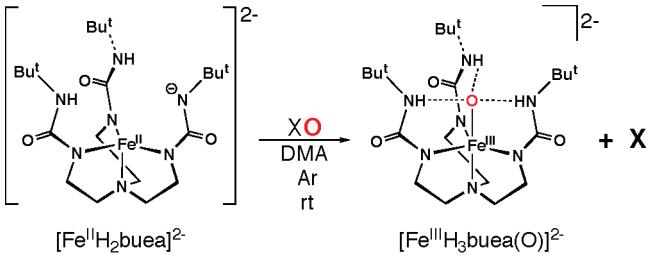

XO = *N*-oxides, hydroxylamines, sulfoxides

FIGURE 5. Reaction of the intermediate $[Fe^{II}H_2buea]^{2-}$ with oxygen-atom transfer reagents.

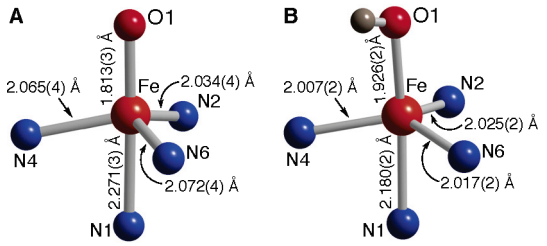

FIGURE 6. Primary coordination spheres and average bond distances for $[Fe^{III}H_3buea(O)]^{2-}$ (A) and $[Fe^{III}H_3buea(OH)]^{-}$ (B).

The role of the basic ureaylate group in the mechanism was probed by evaluating the pK_a value for the Fe^{III}−OH when placed in the H-bond cavity. These studies were done with $[Fe^{III}H_3buea(O)]^{2-}$ and $[Fe^{III}H_3buea(OH)]^{-}$, complexes with fully protonated cavities.[40] A pH titration in DMSO gave a pK_a(Fe−OH) of 25 for $[Fe^{III}H_3buea(OH)]^{-}$. This suggests that a deprotonated α′N^{-} site within the cavity is sufficiently basic (p$K_a \approx 30$) to partake in intramolecular proton transfer for a coordinated hydroxo ligand.

Structural Aspects

Single-crystal X-ray diffraction studies have been done on the potassium salts of $[Fe^{III}H_3buea(O)]^{2-}$ and $[Fe^{III}H_3buea(OH)]^{-}$. Their molecular structures and primary coordination are shown in Scheme 1 and Figure 6, respectively.[37,38] Both complexes have a trigonal bipyramidal coordination geometry, where the trigonal plane is defined by the three αN^{-} atoms from $[H_3buea]^{3-}$. The oxo ligand in $[Fe^{III}H_3buea(O)]^{2-}$ and the hydroxo ligand in $[Fe^{III}H_3buea(OH)]^{-}$ are positioned trans to the apical nitrogen. The Fe−O1 distance of 1.813(3) Å in $[Fe^{III}H_3buea(O)]^{2-}$ is shorter than the 1.931(3) Å distance found in the Fe^{III}−OH complex. In addition, the Fe−N1 length of 2.280(3) Å in $[Fe^{III}H_3buea(O)]^{2-}$ is more than 0.1 Å longer than that in $[Fe^{III}H_3buea(OH)]^{-}$ (Table 1). These results are consistent with the oxo anion being a stronger trans-influencing ligand than hydroxide. In $[Fe^{III}H_3buea(O)]^{2-}$, the N_{urea}−Fe−N_{urea} angles are nearly the same (∼117°), while in $[Fe^{III}H_3buea(OH)]^{-}$ these angles are significantly different (e.g., N2−Fe−N4 = 128.2°; N2−Fe−N6 = 109.4°). These large angular differences in $[Fe^{III}H_3buea(OH)]^{-}$ lead to a more distorted cavity structure resulting from the placement of the O−H vector between the two urea groups. Thus, the cavity can flex to accommodate nonspherical ligands, such a hydroxide. Solution electron paramagnetic resonance (EPR) measurements corroborate the structural differences between $[Fe^{III}H_3buea(O)]^{2-}$ and $[Fe^{III}H_3buea(OH)]^{-}$, the Fe^{III}−OH complex having a significantly more rhombic signal.

The H-bonds within the cavities that surround the Fe^{III}−O(H) units in $[Fe^{III}H_3buea(O)]^{2-}$ and $[Fe^{III}H_3buea(OH)]^{-}$ are formed by the urea groups of the $[H_3buea]^{3-}$ ligand. The molecular structures of $[Fe^{III}H_3buea(O)]^{2-}$ and $[Fe^{III}H_3buea(OH)]^{-}$ reveal that the three α′NH groups are directed toward the oxygen atoms. The observed O···N_{urea} distances are indicative of intramolecular H-bonding between the oxygen atom and the α′NH groups (Table 1).

This description of intramolecular H-bonding in $[Fe^{III}H_3buea(O)]^{2-}$ and $[Fe^{III}H_3buea(OH)]^{-}$ is consistent with solid-state Fourier transform infrared (FTIR) spectroscopic studies that show each complex has a broad peak for the ν(NH) signals centered at ∼3100 cm^{-1}. Density functional theory was also used to analyze the placement of the H-bonds in $[Fe^{III}H_3buea(O)]^{2-}$; calculations at the B3LYP/6-31+G* level of theory evaluated the placement of a proton between the oxo ligand and one of the α′N groups.[38] The calculations produced a double-well energy profile where the FeO···Hα′N description of the H-bond with a discrete Fe^{III}-oxo unit is nearly 7 kcal/mol lower in energy than the Fe(III)−OH tautomer with an FeOH···α′N^{-} interaction. In addition, the optimized structure for the FeO···Hα′N unit gave an Fe^{III}−O distance of 1.802 Å, agreeing with the 1.813 Å value obtained by X-ray diffraction methods. In contrast, the optimized structure for the FeOH···α′N^{-} complex gave an Fe^{III}−O(H) distance of 1.883 Å, a value significantly longer than that observed experimentally.[38]

Table 1. Bond Lengths (Å) for $[M^{III}H_3buea(O)]^{2-}$ and $[M^{III}H_3buea(OH)]^{-}$ [a]

complex	M−O1	M−N1	O···α′N
$[Fe^{III}H_3buea(O)]^{2-}$	1.813(2)	2.276(4)	2.711(6)
$[Fe^{III}H_3buea(OH)]^{-}$	1.926(1)	2.180(2)	2.833(2)
$[Mn^{III}H_3buea(O)]^{2-}$	1.771(4)	2.144(5)	2.731(5)
$[Mn^{III}H_3buea(OH)]^{-}$	1.872(2)	2.033(3)	2.849(3)

[a] Two independent anions are in the asymmetric unit for the complexes; average values are given.

Formation of $[Mn^{III}buea(O)]^{2-}$ and $[Mn^{III}H_3buea(OH)]^{-}$

The analogous Mn^{III}−O(H) complexes, $[Mn^{III}H_3buea(O)]^{2-}$ and $[Mn^{III}H_3buea(OH)]^{-}$, have been isolated using procedures similar to those shown in Scheme 1.[38,41] Like the Fe^{III}−O(H) complexes, these manganese complexes are high-spin ($S = 2$ ground states) with trigonal bipyramidal coordination geometries. A comparison of some structural parameters for the M^{III}−O(H) (M = Fe and Mn) complexes are presented in Table 1, showing similar trends for the M−O(H) and M−N1 bond distances between the iron and manganese complexes.

Nature of the M^{III}−O Interactions

Stable oxometal complexes are generally believed to have multiple bonds between a metal ion and a terminal oxo ligand.[38] Because of this requirement, nearly all complexes with M−O units involve early transition metal ions in high oxidation states. In the mid-1980s, Mayer illustrated that C_3-symmetric, low-spin oxorhenium complexes with d^4 and d^6 electron configurations can support terminal oxo ligation.[42,43] Since these studies, terminal oxo complexes of Ir^{III} and Ru^{IV} have been structurally characterized;[44,45] these complexes too are low-spin, and the recently reported Fe^{IV}═O complexes have $S = 1$ ground states.[46] In fact, other than our $[M^{III}H_3buea(O)]^{2-}$ complexes (M^{III}

= Fe and Mn), there are no examples of discrete high-spin metal complexes with a terminal oxo ligand *and* at least four d electrons. Thus preparation of $[M^{III}H_3buea(O)]^{2-}$ provided an opportunity to evaluate the bonding interaction(s) within M−O units for high-spin complexes of 3d metal ions.

DFT calculations at the B3LYP/6-31G(d,f) level showed a number of different molecular orbitals that contribute to the M^{III}−O bonds in the $[M^{III}H_3buea(O)]^{2-}$ complexes.[38] The bonding description is complicated because none of these molecular orbitals have pure metal-oxo character: each has substantial electron density at different locations throughout the complexes. Further studies using natural bond order analyses suggested that single bonds are the best representations for the M^{III}−O interactions. While this bonding description is unusual (vide supra),[47,48] it is consistent with the magnetic, spectroscopic, and structural properties of the complexes, such as their high-spin ground states, low M−O vibrations, and relatively long M^{III}−O bonds.

H-Bonds and Metal Oxo Complexes

The confinement of the M^{III}−O units within rigid H-bond cavities is one obvious difference between the $[M^{III}H_3buea(O)]^{2-}$ complexes and other oxometal systems. The multiple intramolecular H-bonds undoubtedly affect properties of the complexes, including the M^{III}−O bonding and distances. Strong intramolecular H-bonds to the M−O unit should lessen the π-basicity of the oxo ligands, which in turn would lead to a reduction in metal oxo bond order (i.e., few π-bonds) and longer bond distances—predictions consistent with our findings for the $[M^{III}H_3buea(O)]^{2-}$ and $[M^{II/III}H_3buea(OH)]^{2-/-}$ complexes.

The possibility that H-bonds can modulate the properties of metal oxo complexes would have profound implications particularly in metalloproteins, where H-bond networks are prevalent within active sites. Varying the number or type of H-bonds to a M−O(H) unit could modulate reactivity to ensure a desired function. For instance, multiple H-bonds to a metal oxo center may contribute to its cleaving C−H bonds, whereas a lower number could promote oxygen-atom transfer processes. Similarly, results from structural biology show that numerous hydrolytic metalloenzymes have H-bond networks surrounding the M−OH unit that may produce "hybrid" metal hydroxo centers with enhanced reactivity.

Water as the Source of the Oxo and Hydroxo Ligands

The mechanism for production of $[Fe^{III}H_3buea(O)]^{2-}$ in Figure 2 proposes an anionic site within the H-bond cavity that assists in the formation of the $[M^{III}H_3buea(O)]^{2-}$ complex. This concept led us to prepare M−O(H) complexes directly from water as shown in Figure 7A;[49−51] we envisage this process to occur by the conversion of water to hydroxide with concomitant protonation of the α′N^- group to restore its ability to donate an H-bond. As outlined in Scheme 2 for $[Mn^{II}H_3buea(OH)]^{2-}$, monomeric

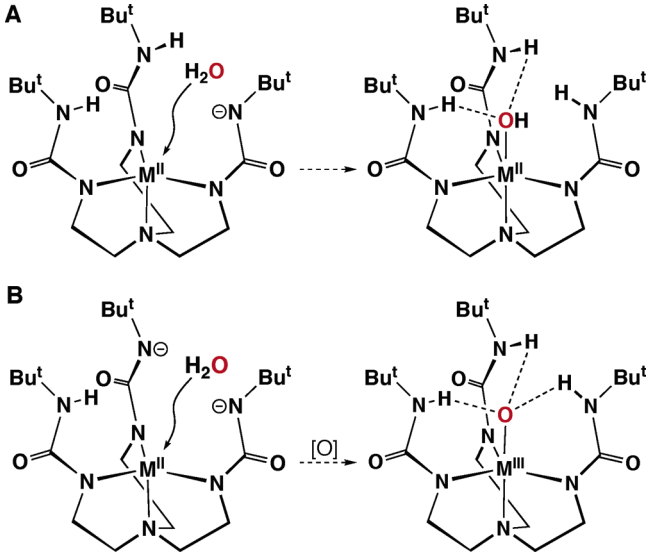

FIGURE 7. Proposed role of the cavity in formation of $[M^{II}H_3buea(OH)]^{2-}$ (A) and $[M^{III}H_3buea(O)]^{2-}$ (B) from water.

complexes with M^{II}−OH motifs (M^{II} = Co, Fe, Mn, and Zn) have been prepared. All the $[M^{II}H_3buea(OH)]^{2-}$ complexes were obtained in relatively high yields after recrystallization. Each complex has the expected trigonal bipyramidal coordination geometry with the M^{II}−OH unit placed within the cavities (Scheme 2). The O−H vectors reside between two of the urea scaffolds, causing distortions in the cavities similar to those observed for $[Fe^{III}H_3buea(OH)]^-$. The Co^{II}−OH, Mn^{II}−OH, and Fe^{II}−OH complexes have relatively negative $M^{III/II}$−OH redox couples (less than −0.50 V vs SCE), allowing for the convenient preparation of the corresponding Co^{III}−OH, Fe^{III}−OH, and Mn^{III}−OH complexes. $[Fe^{III}H_3buea(O)]^{2-}$

Scheme 2. Preparative Routes and Molecular Structures for $[Mn^{II}H_3buea(OH)]^{2-}$, $[Mn^{III}H_3buea(OH)]^-$, and $[Mn^{III}H_3buea(O)]^{2-}$ from Water[a]

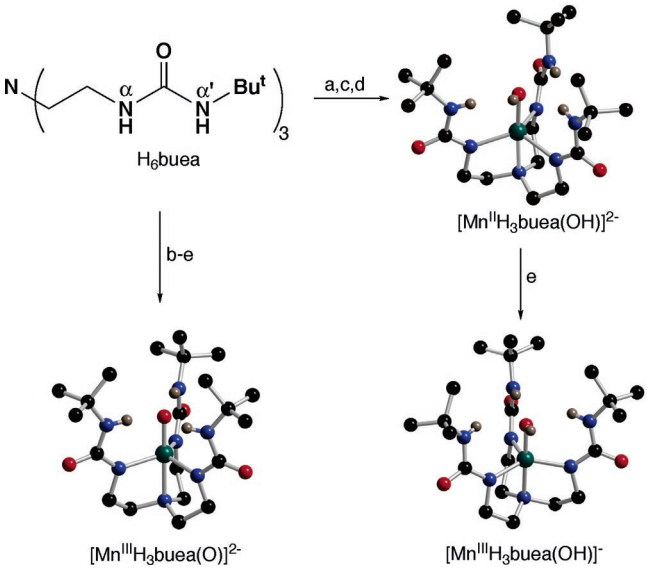

[a] Potassium counterions have been omitted. Conditions: (a) 4 equiv KH, DMA, inert atmosphere (Ar), rt; (b) 5 equiv KH, DMA, Ar, rt; (c) $Mn(OAc)_2$, DMA, Ar, rt; (d) 1 equiv H_2O, rt; (e) 0.5 equiv of O_2 or I_2 or 1.0 equiv of Cp_2Fe^+, DMA, rt.

and $[Mn^{III}H_3buea(O)]^{2-}$ were also synthesized directly from water when two anionic sites are placed within the cavity (Figure 7B and Scheme 2). This methodology permitted the isolation of a unique series of monomeric iron and manganese complexes containing $M^{II/III}$−OH and M^{III}−O units, all with the same primary and secondary coordination spheres.

O−H Bond Dissociation Energies and Chemical Reactivity

The homolytic BDE_{OH}'s of the $M^{II/III}$−OH complexes were evaluated as a prelude to investigating the reactivity of the M^{III}−O complexes.[40] Other researchers[39,52] have shown that BDE_{OH}'s are good predictors for hydrogen atom abstraction processes.[53] Two thermochemical cycles were developed that relied on measuring the $M^{III/II}$−OH and $M^{IV/III}$−O redox potentials and pK_a(M−O*H*) values for the M^{III}−OH complexes in DMSO. We obtained BDE_{OH}'s of 77(4) kcal/mol for $[Mn^{II}H_3buea(O-H)]^{2-}$ and 66(4) kcal/mol for $[Fe^{II}H_3buea(O-H)]^{2-}$, while $[Mn^{III}H_3buea(O-H)]^{-}$ and $[Fe^{III}H_3buea(O-H)]^{-}$ have BDE_{OH}'s of 110(4) and 115(4) kcal/mol, respectively. The BDE_{OH}'s for the M^{III}−OH complexes are sufficiently large to make their corresponding M^{IV}=O complexes exceptionally strong

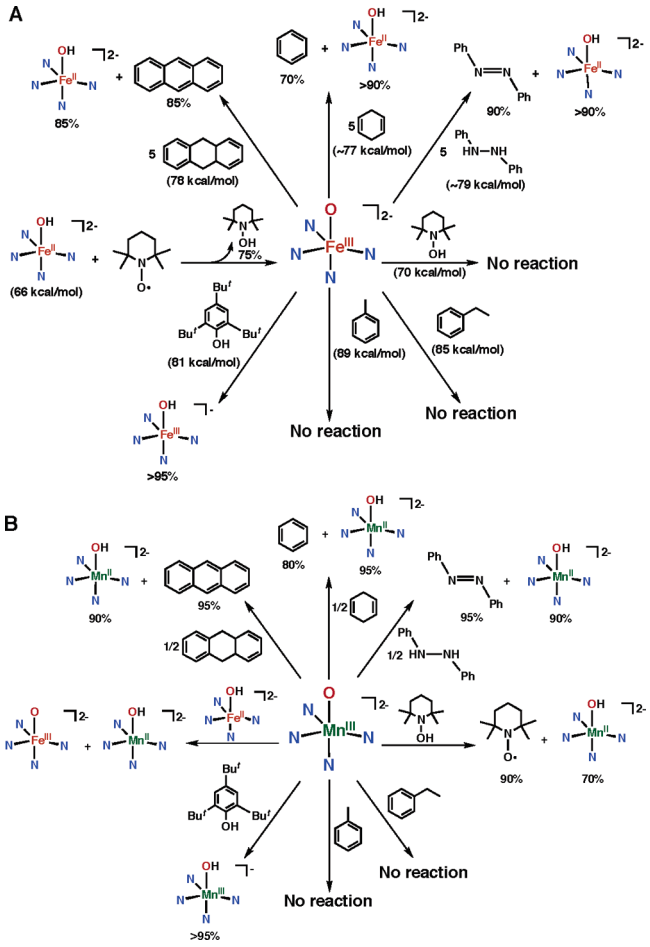

FIGURE 8. Reactivity of $[M^{III}H_3buea(O)]^{2-}$ (M^{III} = Fe (A) and Mn (B)). The metal complexes are represented by their primary coordination spheres, and the values in parentheses are the BDE_{X-H}'s of the substrates.

Scheme 3. Preparative Route and Molecular Structure for $[Co^{III}(H_2bade)(O)]_2^{2-}$ [a]

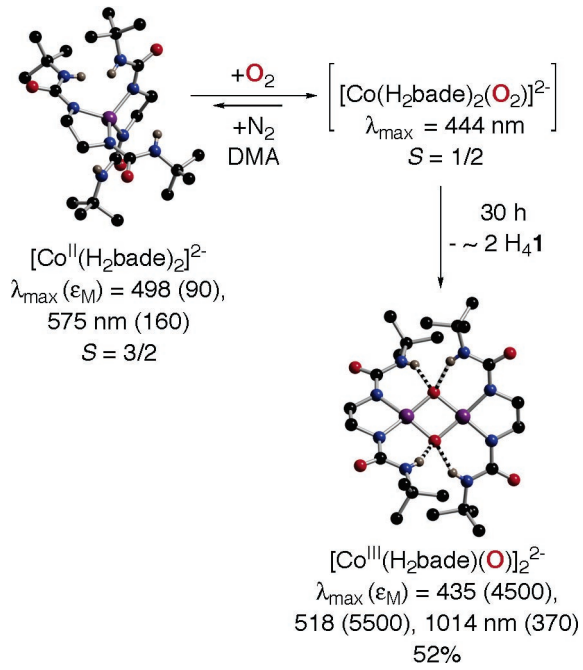

[a] Potassium counterions have been omitted.

H-atom abstractors, comparable to species such as hydroxyl radical (BDE_{OH} = 119 kcal/mol in DMSO).[39] The large affinity of the M^{IV}=O species for H-atoms may explain why their isolation has so far eluded us.

The BDE_{OH}'s were evaluated further with reactivity studies involving substrates having known X−H bond energies. These studies are summarized in Figure 8. In agreement with our BDE_{OH} estimations, $[Fe^{III}H_3buea(O)]^{2-}$ and $[Mn^{III}H_3buea(O)]^{2-}$ react with a variety of substrates having X−H bond strengths less than 80 kcal/mol. For instance, treating the M^{III}−O complexes with either 9,10-dihydroanthracene or 1,4-cyclohexadiene in DMSO at room temperature gave $[M^{II}H_3buea(OH)]^{2-}$ and the dehydrogenated products, anthracene and benzene, in yields of greater than 80%. In general, the reactions with $[Fe^{III}H_3buea(O)]^{2-}$ require an excess of substrate and are slower than those with $[Mn^{III}H_3buea(O)]^{2-}$; both observations are consistent with O−H bond formation in the iron complex being energetically less favorable than that in the manganese system. We also found that proton, rather than H-atom, transfer is observed when $[Mn^{III}H_3buea(O)]^{2-}$ and $[Fe^{III}H_3buea(O)]^{2-}$ are treated with phenolic compounds: the major products are the M^{III}−OH complexes, $[Mn^{III}H_3buea(OH)]^{-}$ and $[Fe^{III}H_3buea(OH)]^{-}$. We have argued that the high basicity of the terminal oxo ligands makes protonation a more likely process.

Open Sesame: H-Bond-Supported Oxo Bridges

We recently developed other multidentate ligands that produce less-constrained H-bond frameworks.[54−56] Metal complexes of these ligands are also being used to probe dioxygen activation: the more open structures should produce metal complexes with a different arrangement

of dioxygen-derived ligands. This is illustrated in Scheme 3 for the dioxygen chemistry of $[Co^{II}(H_2bade)_2]^{2-}$ ($[H_2bade]^{2-}$ = bis[(*tert*-butyl)amino-carbonyl]-1,2-diaminatoethane).[54] This tetrahedral, high-spin Co^{II} complex reacts with an excess of dioxygen to initially form a species with new optical properties and a ground spin state of $S = {}^1/_2$, indicative of a cobalt−dioxygen adduct. However, at room temperature this complex is not stable: it converts to the $[Co^{III}(\mu\text{-}O)_2Co^{III}]$ complex, $[Co^{III}bade(O)]_2^{2-}$, the oxo ligands of which are derived directly from the cleavage of dioxygen.

The molecular structure of $[Co^{III}bade(O)]_2^{2-}$ (Scheme 3) is a rare example of a cobalt dimer containing a $[Co^{III}(\mu\text{-}O)_2Co^{III}]$ rhomb; each Co^{III} center is four-coordinate with a distorted square planar geometry. In addition, the oxo ligands participate in two intramolecular H-bonds with the α′NH groups of $[H_2bade]^{2-}$. We proposed that this distinctive H-bond network, coupled with the anion ligand field around the cobalt centers, sufficiently stabilizes the $[Co^{III}(\mu\text{-}O)_2Co^{III}]$ core at room temperature to allow isolation of the complex. The thermal stability of $[Co^{III}bade(O)]_2^{2-}$ contrasts with that found for $[M^{III}(\mu\text{-}O)_2M^{III}]$ rhombs of most other late 3d transition metals, which are only stable at temperatures below −20 °C.[57,58]

Summary and Prospects

The importance of the secondary coordination sphere in metal complexes has been recognized since the time of Werner.[59] Renewed interest in this concept has come from structural biology, where H-bonds in the active sites of metalloproteins are touted as essential components for function. The systems described in this Account offer an approach to designing bioinspired metal complexes having rigid organic frameworks with H-bond donors. Several new complexes have been generated through dioxygen activation, including $[Fe^{III}H_3buea(O)]^{2-}$, the first structurally characterized iron complex with a terminal oxo ligand. Reactivity studies with oxygen-atom transfer agents implicate an Fe^{IV}═O intermediate being formed along the reaction path; however, this species has not yet been observed. Our inability to isolate the Fe^{IV}═O complex may be related to the large thermodynamic driving force that the Fe^{IV}═O complex, $[Fe^{IV}H_3buea(O)]^-$, has for hydrogen atoms. Furthermore, the reactivity of the putative $[Fe^{IV}H_3buea(O)]^-$ is different from that reported for other isolated Fe^{IV}═O complexes,[35] underscoring our view that higher valent oxoiron complexes can have a range of reactivities.

The picture emerging for $[Fe^{III}H_3buea(O)]^{2-}$ and $[Mn^{III}H_3buea(O)]^{2-}$ is a departure from the classical descriptions of oxometal complexes. The presence of three H-bond donors around the M^{III}−O units in $[M^{III}H_3buea(O)]^{2-}$ produces unusual spectroscopic, structural, and bonding properties, supporting the intriguing possibility that H-bonds can be used to regulate function in complexes with terminal oxo ligands. The importance of the secondary coordination sphere is further underscored by inclusion of anionic sites within the cavities (via deprotonation of the α′NH groups), which was instrumental in formation of $[M^{III}H_3buea(O)]^{2-}$ from dioxygen and the $M^{II/III}$−OH and M^{III}−O complexes from water.

Additionally studies are clearly needed to fully understand the effects of H-bonds on the stability and reactivity of metal complexes. H-bonds will also influence other metal-based reactions, including transformations not found in biology.[60] For instance, we recently prepared $[Fe^{III}H_3buea(E)]^{2-}$ complexes, where E represents terminal sulfido and selenido ligands, by routes analogous to that developed for $[Fe^{III}H_3buea(O)]^{2-}$.[61] Integrating these noncovalent interactions within ligand frameworks should enhance the performance of metal-based reagents and catalysts.

Support for this work came from the NIH (Grant GM50781). I have worked with an outstanding group of scientists who performed the work described in this Account; they include C. MacBeth, R. Gupta, P. Larsen, B. S. Hammes, Z. Shirin, M. Zart, M. Ray, M. Miller, K. Mitchell-Koch, M. Hendrich, V. Young, D. Powell, and W. Thompson. I am most grateful for their efforts on this project. This article is dedicated to T. N. Sorrell, who taught me the art and craft of chemical synthesis.

References

(1) Dawson, J. H. Probing Structure−Function relations in Heme-Containing Oxygenases and Peroxidases. *Science* **1988**, *240*, 433−439.
(2) Ortiz de Montellano, P. R. Control of the Catalytic Activity of Prosthetic Heme by the Structure of Hemoproteins. *Acc. Chem. Res.* **1987**, *20*, 289−294.
(3) Holm, R. H.; Kennepohl, P.; Solomon, E. I. Structural and Functional Aspects of Metal Sites in Biology. *Chem. Rev.* **1996**, *96*, 2239−2314.
(4) For recent reviews on biomimetic inorganic chemistry, see: Holm, R. H.; Solomon, E. I. *Chem. Rev.* **2004**, *104*, 347−1200.
(5) Lu, Y.; Valentine, J. S. *Curr. Opin. Struct. Biol.* **1997**, *7*, 495−500.
(6) Etter, M. C. Encoding and Decoding Hydrogen Bond Patterns of Organic Molecules. *Acc. Chem. Res.* **1990**, *23*, 120−126.
(7) Perutz, M. F.; Fermi, G.; Luisi, B.; Shaanan, B.; Liddington, R. C. Stereochemistry of Cooperative Mechanism in Hemoglobin. *Acc. Chem. Res.* **1987**, *20*, 309−321.
(8) Springer, B. A.; Sligar, S. G.; Olsen, J. S.; Philips, G. N., Jr. Mechanism of Ligand Recognition in Myoglobin. *Chem. Rev.* **1994**, *94*, 699−714.
(9) Gerber, N. C.; Sligar, S. G. Catalytic Mechanism of Cytochrome P-450: Evidence for a Distal Charge Relay. *J. Am. Chem. Soc.* **1992**, *114*, 8742−8743.
(10) Sono, M.; Roach, M. P.; Coulter, E. D.; Dawson, J. H. Heme-Containing Oxygenases. *Chem. Rev.* **1996**, *96*, 2841−2887.
(11) Mukai, M.; Nagano, S.; Tanaka, M.; Ishimori, K.; Morishima, I.; Ogura, T.; Watanabe, Y.; Kitagawa, T. Effects of Concerted Hydrogen Bonding of Distal Histidine on Active Site Structures of Horseradiah Peroxidase. Resonance Ramon Studies with Asn70 Mutants. *J. Am. Chem. Soc.* **1997**, *119*, 1758−1766.
(12) Fülöp, V.; Phizackerley, R. P.; Soltis, S. M.; Clifton, I. J.; Wakatuski, S.; Erman, J.; Hajdu, J.; Edwards, S. L. Laue Diffraction Study on the Structure of Cytochrome *c* Peroxidase Compound I. *Structure* **1994**, *2*, 201−208.
(13) Ozaki, S.-i.; Roach, M. P.; Matsui, T.; Watanabe, Y. Investigations of the Roles of the Distal Heme Environment and the Proximal Heme Iron Ligand in Peroxide Activation by Heme Enzymes via Molecular Engineering of Myoglobin. *Acc. Chem. Res.* **2001**, *34*, 818−825.
(14) Vance, C. K.; Miller, A.-F. Novel Insights into the Basis for *Escherichia coli* Superoxide Dismutase's Metal Ion Specificity from Mn-Substituted FeSOD and Its Very High E_m. *Biochemistry* **2001**, *40*, 13079−13087.
(15) Xie, J.; Yikilmaz, E.; Miller, A.-F.; Brunold, T. C. Second Sphere Contributions to Substrate-Analogue Binding in Iron(III) Superoxide Dismutase. *J. Am. Chem. Soc.* **2002**, *124*, 3769−3774.
(16) Edward, R. A.; Whittaker, M. M.; Whittaker, J. M.; Baker, E. N.; Jameson, G. B. Outer Sphere Mutations Perturb Metal Reactivity in Manganese Superoxide Dismutase. *Biochemistry* **2001**, *40*, 15−27.

(17) Tomchick, D. R.; Phan, P.; Cymborowski, M.; Minor, W.; Holman, T. R. Structural and Functional Characterization of Second-Coordination Sphere Mutants of Soybean Lipoxygenase-1. *Biochemistry* **2001**, *40*, 7509−7517.

(18) Du Bois, J.; Mizoguchi, T. J.; Lippard, S. J. Understanding the dioxygen reaction chemistry of diiron proteins through synthetic modeling studies. *Coord. Chem. Rev.* **2000**, *200*−*202*, 443−485.

(19) Momenteau, M.; Reed, C. A. Synthetic Heme Dioxygen Models. *Chem. Rev.* **1994**, *94*, 659−698.

(20) Collman, J. P.; Zhang, X.; Wong, K.; Brauman, J. I. Dioxygen Binding in Iron and Cobalt Picnic Basket Porphyrins. *J. Am. Chem. Soc.* **1994**, *116*, 6245−6251.

(21) Yeh, C.-Y.; Chang, C. J.; Nocera, D. G. Hangman's Porphyrins for the Assembly of a Model Heme Water Channel. *J. Am. Chem. Soc.* **2001**, *123*, 1513−1514.

(22) Rudkevich, D. M.; Verboom, W.; Brzozka, Z.; Palys, M. J.; Stauthamer, W. P. R. V.; van Hummel, G. J.; Franken, S. M.; Harkema, S.; Engbersen, J. F. J.; Reinhoudt, D. N. Functionalized UO_2 Salenes: Neutral Receptors for Anions. *J. Am. Chem. Soc.* **1994**, *116*, 4341−4351.

(23) Walton, P. H.; Raymond, K. N. Stereognostic Coordination Chemistry 4: The Design and Synthesis of a Selective Uranyl Ion Complexant. *Inorg. Chim. Acta* **1995**, *240*, 593−601.

(24) Kickham, J. E.; Loeb, S. L.; Murphy, S. L. Molecular Recognition of Nucleobases via Simultaneous First- and Second-Sphere Coordination. *J. Am. Chem. Soc.* **1993**, *115*, 7031−7032.

(25) Ogo, S.; Wada, S.; Watanabe, Y.; Iwase, M.; Wada, A.; Harata, M.; Jitsukawa, K.; Masuda, H.; Einage, H. Synthesis, Structure, and Spectroscopic Properties of $[Fe^{III}(tnpa)(OH)(PhCOO)]ClO_4$. *Angew. Chem., Int. Ed.* **1998**, *37*, 2101−2104.

(26) Garner, D. K.; Allred, R. A.; Tubbs, K. J.; Arif, A. M.; Berreau, L. M. Synthesis and Characterization of Mononuclear Zinc Aryloxide Complexes Supported by Nitrogen/Sulfur Ligands Possessing an Internal Hydrogen Bond Donor. *Inorg. Chem.* **2002**, *41*, 3533−3541.

(27) Garner, D. K.; Fitch, S. B.; McAlexander, L. H.; Bezold, L. M.; Arif, A. M.; Berreau, L. M. Mononuclear Nitrogen/Sulfur-Ligated Zinc Methoxide and Hydroxide Complexes: Investigating Ligand Effects on the Hydrolytic Stability of Zinc Alkoxide Species. *J. Am. Chem. Soc.* **2002**, *124*, 9970−9971.

(28) Kitajima, N.; Komatsuzaki, H.; Hikichi, S.; Osawa, M.; Moro-oka, Y. A Monomeric Side-On Peroxo Manganese(III) Complex: $Mn(O_2)(3,5\text{-}^iPr_2pzH)(HB(3,5\text{-}^iPr_2pz)_3)$. *J. Am. Chem. Soc.* **1994**, *116*, 11596−11597.

(29) Hammes, B. S.; Luo, X.; Carrano, M. W.; Carrano, C. J. Guest Preorganization: An Alternative Bioinspired Paradigm in Host−Guest Chemistry. *Angew. Chem., Int. Ed.* **2002**, *41*, 2166−2167.

(30) Cheruzel, L. E.; Wang, J. P.; Mashuta, M. S.; Buchanan, R. M. Structure and Properties of an Fe(III) Complex Containing a Novel Amide Functionalized Polyimidazole Ligand. *Chem. Commun.* **2002**, 2166−2167.

(31) Bordwell, F. G.; Fried, H. G.; Hughs, D. L.; Lynch, T. Y.; Satish, A. V.; Whang, Y. E. Acidities of Carboxamides, Hydroxamic Acids, Carbohydrazides, Benzenesulfonamides, and Benzenesulfonohydrazides in DMSO Solution. *J. Org. Chem.* **1990**, *55*, 3330−3336.

(32) Margerum, D. W. Metal Peptide Complexes. *Pure Appl. Chem.* **1983**, *55*, 23−34.

(33) Collins, T. J. Designing Ligands for Oxidizing Complexes. *Acc. Chem. Res.* **1994**, *27*, 279−285.

(34) Hopper, M. L.; Schlemper, E. O.; Murmann, R. K. Structure of Dipotassium Ferrate(VI). *Acta Crystallogr.* **1982**, *B32*, 2237−2240.

(35) Rohde, J.-U.; In, J.-H.; Lim, M. H.; Brennessel, W. W.; Bukowski, M. R.; Stubna, A.; Muenck, E.; Nam, W.; Que, L., Jr. Crystallographic and Spectroscopic Characterization of a Nonheme Fe(IV)=O Complex. *Science* **2003**, *299*, 1037−1039.

(36) Costas, M.; Mehn, M. P.; Jensen, M. P.; Que, L., Jr. Dioxygen Activation at Mononuclear Nonheme Iron Active Sites: Enzymes, Models, and Intermediates. *Chem. Rev.* **2004**, *104*, 939−986.

(37) MacBeth, C. E.; Golombek, A. P.; Young, V. G., Jr.; Yang, C.; Kuczera, K.; Hendrich, M. P.; Borovik, A. S. O_2 Activation by Nonheme Iron Complexes: A Monomeric Fe(III)-oxo Complex Derived from O_2. *Science* **2000**, *289*, 938−941.

(38) MacBeth, C. E.; Gupta, R.; Mitchell-Koch, K. R.; Young, V. G., Jr.; Lushington, G. H.; Thompson, W. H.; Hendrich, M. P.; Borovik, A. S. Utilization of Hydrogen Bonds To Stabilize M−O(H) Units: Synthesis and Properties of Monomeric Iron and Manganese Complexes with Terminal Oxo and Hydroxo Ligands. *J. Am. Chem. Soc.* **2004**, *126*, 2556−2567.

(39) Mayer, J. M. Hydrogen Atom Abstraction by Metal-Oxo Complexes: Understanding the Analogy with Organic Radical Reactions. *Acc. Chem. Res.* **1998**, *31*, 441−450.

(40) Gupta, R.; Borovik, A. S. Monomeric $Mn^{III/II}$ and $Fe^{III/II}$ Complexes with Terminal Hydroxo and Oxo Ligands: Probing Reactivity via O−H Bond Dissociation Energies. *J. Am. Chem. Soc.* **2003**, *125*, 13234−13242.

(41) Shirin, Z.; Hammes, B. S.; Young, V. G., Jr.; Borovik, A. S. Hydrogen Bonding in Metal Oxo Complexes: Synthesis and Structure of a Monomeric Manganese(III)-Oxo Complex and Its Hydroxo Analogue. *J. Am. Chem. Soc.* **2000**, *122*, 1836−1837.

(42) Mayer, J. M.; Thorn, D. L.; Tulip, T. H. Synthesis, Reactions, and Electronic Structure of Low-Valent Rhenium-Oxo Compounds. Crystal and Molecular Structure of $Re(O)I(MeC{=}CMe)_2$. *J. Am. Chem. Soc.* **1985**, *107*, 7454−7462.

(43) Spaltenstein, E.; Conry, R. R.; Critchlow, S. C.; Mayer, J. M. Low-Valent Rhenium-Oxo Complexes. 9. Synthesis, Characterization, and Reactivity of a Formally Rhenium(I) Terminal Oxo Complex, $NaRe(O)(RC{=}CR)_2$. *J. Am. Chem. Soc.* **1989**, *111*, 8741−8742.

(44) Hay-Motherwell, R. S.; Wilkinson, G.; Hussain-Bates, B.; Hursthouse, M. B. Synthesis and X-ray Crystal Structure of Oxotrimesityliridium(V). *Polyhedron* **1993**, *12*, 2009−2012.

(45) Welch, T. W.; Ciftan, S. A.; White, P. S.; Thorp, H. H. Electron-Rich Oxoruthenium(IV) Cleavage Agents: A Zero-Order Rate Law for DNA Catalysis. *Inorg. Chem.* **1997**, *36*, 4812−4821.

(46) Decker, A.; Rohde, J.-U.; Que, L., Jr.; Solomon, E. I. Spectroscopic and Quantum Chemical Characterization of the Electronic Structure and Bonding in a Non-Heme Fe^{IV}=O Complex. *J. Am. Chem. Soc.* **2004**, *126*, 5378−5379.

(47) Nugent, W. A.; Mayer, J. M. *Metal*−*Ligand Multiple Bonds: the Chemistry of Transition Metal Complexes Containing Oxo, Nitrido, Imido, Alkylidene, or Akylidyne Ligands*, 1st ed.; Wiley: New York, 1988.

(48) Holm, R. H. Metal-Centered Oxygen Atom Transfer Reactions. *Chem. Rev.* **1987**, *87*, 1401−1449.

(49) Hammes, B. S.; Young, V. G., Jr.; Borovik, A. S. Hydrogen-Bonding Cavities about Metal Ions: a Redox Pair of Coordinatively Unsaturated Paramagnetic Co−OH Complexes, *Angew. Chem., Int. Ed.* **1999**, *38*, 666−669.

(50) MacBeth, C. E.; Hammes, B. S.; Young, V. G., Jr.; Borovik, A. S. Hydrogen-Bonding Cavities about Metal Ions: Synthesis, Structure, and Physical Properties for a Series of Monomeric M-OH Complexes Derived from Water. *Inorg. Chem.* **2001**, *40*, 4733−4741.

(51) Gupta, R.; MacBeth, C. E.; Young, V. G., Jr.; Borovik, A. S. Isolation of Monomeric $Mn^{III/II}$−OH and Mn^{III}−O Complexes from Water: Evaluation of O−H Bond Dissociation Energies. *J. Am. Chem. Soc.* **2002**, *124*, 1136−1137.

(52) Bordwell, F. G.; Cheng, J.; Ji, G.-Z.; Satish, A. V.; Zhang, X. Bond Dissociation Energies in DMSO Related to the Gas Phase. *J. Am. Chem. Soc.* **1991**, *113*, 9790−9795.

(53) Caudle, M. T.; Pecoraro, V. L. Thermodynamic Viability of Hydrogen Atom Transfer from Water Coordinated to the Oxygen-Evolving Complex of Photosystem II. *J. Am. Chem. Soc.* **1997**, *119*, 3415−3416.

(54) Larsen, P. L.; Parolin, T. J.; Powell, D. R.; Hendrich, M. P.; Borovik, A. S. Hydrogen Bonds Around $M(\mu\text{-}O)_2M$ Rhombs: Stabilizing a $[Co^{III}(\mu\text{-}O)_2Co^{III}]$ Complex at Room Temperature. *Angew. Chem., Int. Ed.* **2003**, *42*, 85−89.

(55) MacBeth, C. E.; Larsen, P. L.; Sorrell, T. N.; Powell, D.; Borovik, A. S. A Bidentate Ligand with Appended Hydrogen Bond Donors: Synthesis and Structure of Four-Coordinate Metal Complexes with Bis[(*tert*-butyl)aminocarbonyl]-1,2-diaminoethane. *Inorg. Chim. Acta* **2002**, *341*, 77−84.

(56) Zart, M. K.; Sorrell, T. N.; Powell, D.; Borovik, A. S. Development of Bio-Inspired Chelates with Hydrogen Bond Donors: Synthesis and Structure of Monomeric Metal Acetate Complexes with Intramolecular Hydrogen Bonds. *Dalton Trans.* **2003**, 1986−1992.

(57) Que, L., Jr.; Tolman, W. B. Bis-(μ-oxo)dimetal "Diamond" Cores in Copper and Iron Complexes Relevant to Biocatalysis. *Angew. Chem., Int. Ed.* **2002**, *41*, 1114−1137.

(58) For a recent example of a room temperature $[Co^{III}(\mu\text{-}O)_2Co^{III}]$ complex, see: Dai, X.; Kapoor, P.; Warren, T. H. $[Me_2NN]Co(\eta^6\text{-}$toluene): O=O, N=N, and O=N Bond Cleavage Provides β-Diketiminato Cobalt μ-Oxo and Imido Complexes. *J. Am. Chem. Soc.* **2004**, *126*, 4798−4799.

(59) Colquhoun, H. M.; Stoddart, J. F.; Williams, D. J. Second-Sphere Coordination-A Novel Role for Molecular Receptors. *Angew. Chem., Int. Ed. Engl.* **1986**, *25*, 487−507.

(60) Yao, W.; Carbtree, R. H. An η^1-Aldehyde Complex and the Role of Hydrogen Bonding in Its Conversion to an η^1-Imine Complex. *Inorg. Chem.* **1996**, *35*, 3007−3011.

(61) Larsen, P. L.; Gupta, R.; Powell, D. R.; Borovik, A. S. Chalcogens as Terminal Ligands to Iron: Synthesis and Structure of Complexes with Fe^{III}−S and Fe^{III}−Se Motifs. *J. Am. Chem. Soc.* **2004**, *126*, 6522−6523.

AR030160Q